Virchows Arch [Pathol Anat] (1981) 390:161–179

Virchows Archiv A

Supracellular Structural Principle and Geometry of Blood Vessels*

Norio Suwa
Kotakecho 1–33, Nerimaku, Tokyo, Japan 176

Summary. All the supracellular structures of multicellular organisms are subordinate to a single structural principle. It is a particular space division minimizing the potential energy of the constituent units in a field of mechanical force and is specified as equilibrium space division (ESD). Three-dimensional ESD is characterized by the feature that three faces unite to an edge and four edges converge to a corner, but other geometrical characters are susceptible to variation. Blood vessels are localized predominantly on edges of ESD, so that their geometry depends largely on ESD. ESD is represented approximately by a model of complete space division with uniform β-tetrakaidecahedra, and some geometrical parameters of blood vessels can be derived theoretically from ESD, partly with the aid of the above-mentioned model. ESD is a statistical process under incomplete restrictions. It is consequently impossible to interpret the morphogenesis of supracellular structures directly from genetic information in a deterministic manner.

Key words: Random packing – Equilibrium space division – Space-filling polyhedron – Supracellular structural principle – Vascular geometry.

Introduction

In every organ made of compact cell aggregates three borderlines of cells on the histological section converge to a point. The same principle is also followed by larger structural units, including pathological structures, as demonstrated in Fig. 1. This general rule has an important implication, because it suggests the nature of a structural principle which is universally applicable to all the supracellular structures of multicellular organisms, and the present research is nothing but a theoretical development from this simple finding.

In three-dimensional space the general supracellular structural principle is reproduced by a particular space division with membranes characterized by

* The essential part of this paper was presented at the symposium for celebrating the 70th birthday of Prof. J.A. Linzbach in Göttingen on January 19, 1980

0340-1227/81/0390/0161/$03.80

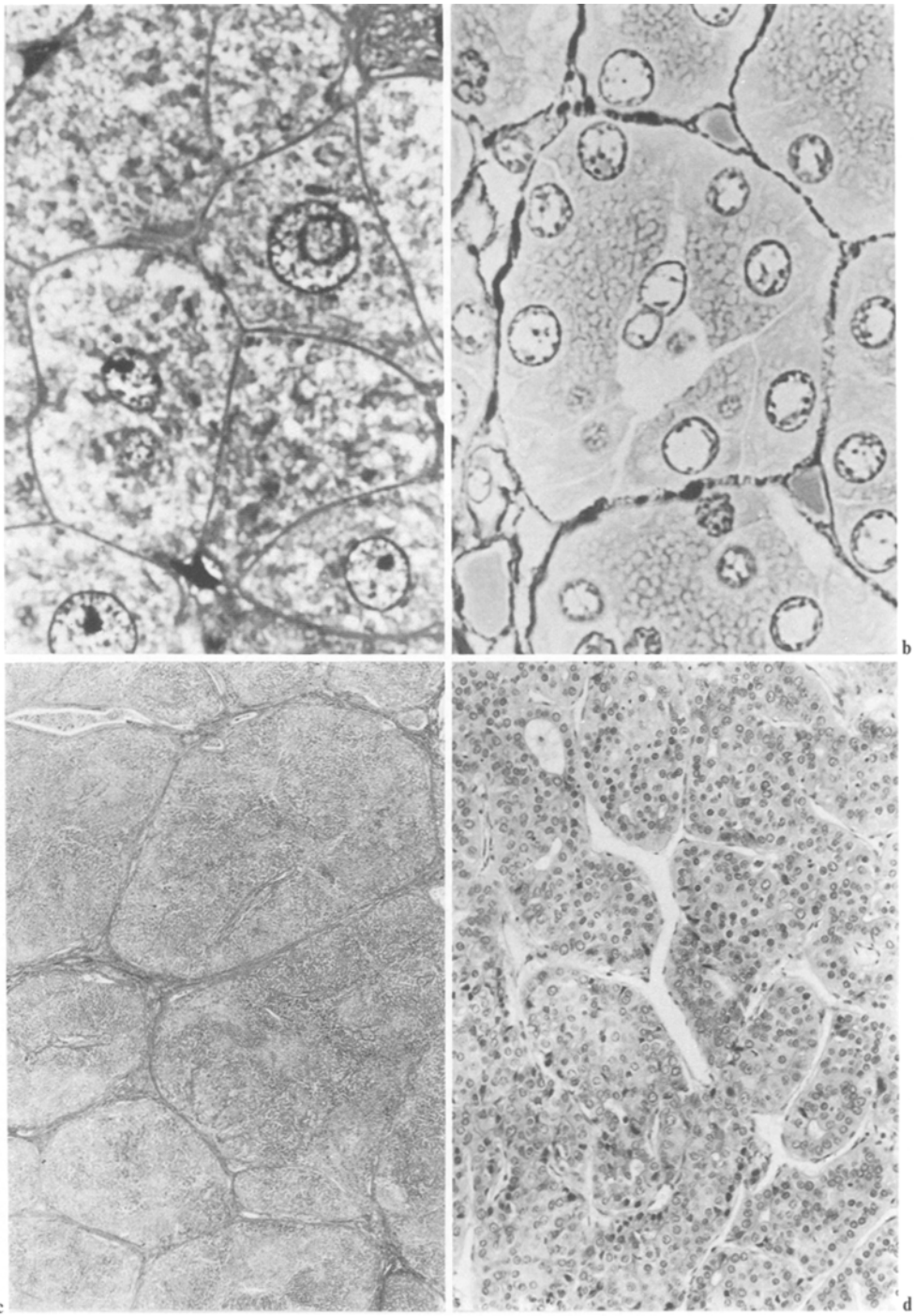

Fig. 1a–d. The general structural principle of cell aggregate and larger units is demonstrated with human autopsy specimens. **a** Upper left. Normal liver cells. **b** Upper right. Normal pancreatic acini. Note capillaries at converging points of three acinar borderlines. **c** Lower left. Liver cirrhosis. Note that three connective tissue septa unite at a point. **d** Lower right. Primary liver cell cancer. Note the blood space making the boundaries of cancer alveoli and convergence of three blood spaces to a point

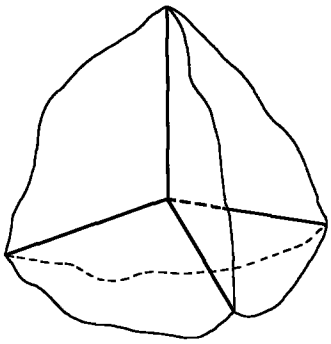

Fig. 2. Essential geometrical features of the space division underlying the appearances of Fig. 1 is demonstrated diagrammatically. Three faces uniting to an edge yield three borderlines converging to a point on a sectional phane

that three faces unite to an edge and four edges converge to a corner. Figure 2 shows its essential geometrical features in the vicinity of a corner. Such a space division appears in a large number of apparently different natural phenomena, which are, however, derived from a common physical law. A classical example is the space division with soap foam, which is not capable of simple mathematical treatment. It seems more practical to consider a model of space division with the Voronoi polyhedra made around randomly packed hard spheres, and its geometry is discussed initially.

Random Packing of Spheres

This expression means a compact aggregate of a large number of hard spheres packed under centripetal force acting uniformly from every direction. The spheres may be of different sizes, but only the case of equal spheres is considered in the present study for the sake of easy theoretical treatment. For example, we can suppose an aggregate of steel balls for ball bearings held tightly in the palm. It is well-known that the spatial arrangement of spheres in this condition is irregular and cannot be reduced to a plan of any elementary sphere groups. In other words the distribution of spheres in the space at any trial of random packing is not reproducible by subsequent trials even with the same sphere sample. The general appearance of random packing is already clear on a relatively small number of spheres as in Fig. 3.

Random packing is accordingly a kind of stochastic process. However, an important restriction is inherent to this particular sphere system: namely, every sphere occupies a certain space into which other spheres cannot enter. This causes a serious deviation in sphere arrangement from a purely stochastic one, especially in compact aggregation. Sphere distribution should be randomized in the statistical sense of the word in a stochastic arrangement. In a random distribution no positional restriction is imposed by any component on others. In this respect, the expression random packing is somewhat misleading. However, there is no other pertinent terminology known for this particular sphere aggregate, so that the conventional term is still used in the present study. Random packing is therefore a stochastic process with the above-mentioned restriction and not strictly congruent with the concept of statistical randomness.

The arrangement of spheres when they are packed tightly by uniform centripetal force inevitably becomes irregular and has to take the form of random packing. This results from the following two requirements. One of them is an isotropic sphere distribution; this requires that the expected number of spheres intersecting a certain test plane must be the same, regardless of the position and direction of the latter in the sphere heap. The other is stable mechanical equilibrium of spheres, which is ensured by a particular configuration that every sphere is fixed in the space in such a way that its possible dislocation in any direction is always stopped by three supporting spheres. The two requirements cannot be simultaneously satisfied by any regular sphere pile, and

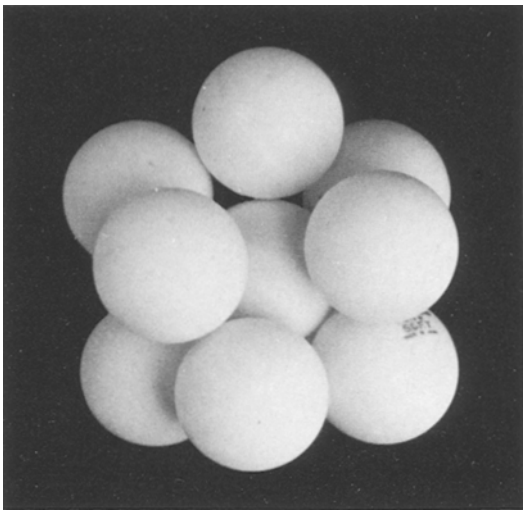

Fig. 3. Randomly packed ping-pong balls are demonstrated. Note their irregular spatial arrangement

random packing is the only possibility which would sustain a three-dimensional sphere aggregate under uniform centripetal force.

Much attention has been recently paid to random packing as a pertinent model for the structure of liquids, and important contributions to the geometry of this particular sphere heap have been made by Bernal (1959, 1964), Bernal and Mason (1960), Finney (1970) and Gotoh and Finney (1974).

Equilibrium Space Division (ESD)

Hard spheres cannot completely fill the three-dimensional space even in the tightest heap. In order to reproduce a complete space division as observed in cell aggregates polyhedra should be constructed in some way from the spheres. There are two different approaches to the problem. In one of them soft spheres are used instead of hard ones, so that they can be compressed and transformed into polyhedra. In the other a plane is inserted between every two adjacent hard spheres in equal distances from them and perpendicular to the line connecting their centers. In the case of two contacting spheres the plane becomes their common tangential plane. The assembly of planes made in this way demarcates a polyhedron around each sphere and completely divides the three-dimensional space. The polyhedron is a kind of the Voronoi polyhedron that defines the region within which every point is situated nearer to the inscribed sphere than to any other one. The two methods would produce space divisions different in their metric properties, but the topological characteristics of cell aggregates and the piles of larger structural units are reproduced equally well. This is due to the particular structure of random packing which produces stable mechanical equilibrium: a sphere is always supported and fixed by three other spheres in every direction.

For biological structures the model of soft spheres would appear to be more easily acceptable, but mathematical derivations of the polyhedra are not simple. In the present study the model of the Voronoi polyhedra around hard

spheres is rather preferable, because it affords a clearer insight into the nature of this particular space division. The mechanical load is carried by the underlying spheres, and the model corresponds to the state of the least potential energy of the sphere system under uniform centripetal force. The space division with the Voronoi polyhedra around randomly packed hard spheres is accordingly a geometrical expression of the second law of thermodynamics. It may be pertinently called "equilibrium space division" or ESD, and the individual Voronoi polyhedra are specified as "polyhedra of ESD".

It should be noted that the supracellular structural principle conforms perfectly to ESD. This finding provides clear evidence that the supracellular structures are entirely subordinate to a field of force extraneous to living cells. The cell is surely not endowed with the ability to prescribe the position of its neighbours in the space. No specific biological activity can be assumed for the supracellular structural principle, and the universal physical law is applicable to the biological structures as well as to inorganic materials.

Because ESD as a general concept is a geometrization of the second law of thermodynamics tending to minimize the potential energy of a certain mechanical system, the form of divided space depends upon the character of the field of force. Three-dimensional space division is possible only under uniform centripetal force. Any polarity in the field of force has an effect of lowering the dimension of the space to be divided and produces two-dimensional or one-dimensional structures. The relations between the dimension of space and the character of force will be discussed later in detail.

In supracellular structures uniform centripetal force is generated mostly by the tension of connective tissue. It may constitute the capsule of an organ, but it plays a more important role as connective tissue septa lobulating the organ. The tension of connecting tissue membranes is coverted to force or pressure acting in the directions perpendicular to the membranes. The situation is the same as in the space division with soap foam, where the surface tension of soap films compresses enclosed air. It is of further interest that connective tissue membranes may be partly deleted without seriously affecting mechanical equilibrium. For example, reconstruction studies of normal pancreatic lobules and cirrhotic livers disclose that their connective tissue septa do not make continuous walls enclosing parenchymal masses. The septa are usually grossly defective and perforated by large parenchymal bridges. Tensile force to maintain three-dimensional sturctures is not then produced so uniformly from connective tissue membranes as surface tension is generated from soap films. The mechanical load is more and more shifted to the limited region around the edges of polyhedra of ESD. From the mechanical viewpoint ESD would be possible only with connective tissue chords localized on the edges of imaginary polyhedra of ESD, provided that parenchymal tissue is cohesive enough. Normal human liver approximately corresponds to this extreme case.

Geometry of Polyhedron of ESD

In this section only three-dimensional ESD is considered. The sole invariable character of an isolated polyhedron of ESD is that every corner is made by

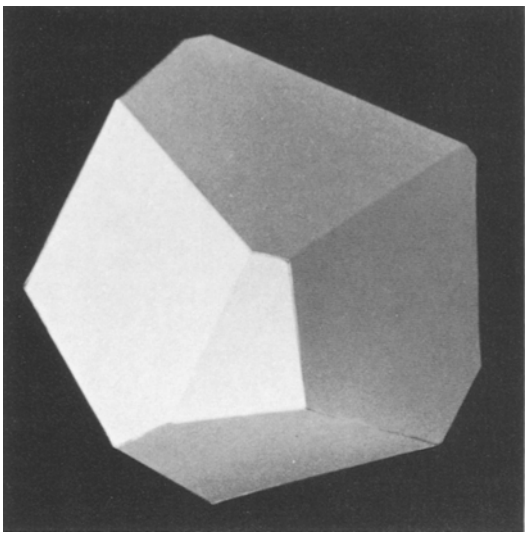

Fig. 4. A polyhedron of ESD made on a mathematical model of random packing is demonstrated. The method consists in a restricted statistical trial to place spheres around a reference sphere and to calculate the Voronoi polyhedron. Note the irregular shape and the invariable topological character that three edges converge to a corner

three converging edges. This is the geometrical expression of stable mechanical equilibrium of spheres underlying the polyhedra, which is established by the presence of three supporting spheres against any one sphere in any direction. All the other geometrical parameters, such as the numbers of faces, edges and corners, are variable and only accessible to statistical treatment. A clear and simple geometrical analysis is consequently impossible. Previous investigations on the shape of the polyhedron were practically limited to direct observations of isolated plant cells or compressed soft metal balls, as those of Dodd (1944), Lewis (1923), Marvin (1939) and Matzke (1939, 1946). Apart from the difficulty often experienced in exactly identifying edges on more or less curved surfaces of natural objects, it is not certain whether these purely empirical approaches would always disclose well-defined ESD susceptible of theoretical consideration or not. In the present study, important geometrical parameters of the polyhedron of ESD are examined on a mathematical model based on experimental statistical trials. Figure 4 shows one of the polyhedra determined with this method.

The distribution of the number of faces examined on 15 polyhedra is as follows.

Number of faces	11	12	13	14	15
Incidence	1	2	4	6	2

The peak of incidence is found at 14; a tetrakaidecahedron appears most frequently. Because the present method needs rather complicated calculations and is therefore time-consuming, there are still only a small number of polyhedra available. Despite the limited number, however, the result is in good agreement with observations on plant cells and also with the already established finding of the space division with soap foam. It is at present difficult to give the exact mean of the number of faces, but it would be very close to 14.

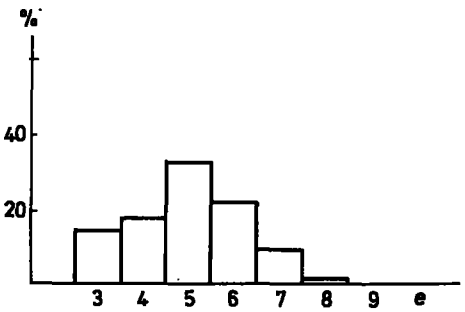

Fig. 5. Distribution of the number e of the sides on a face of the polyhedron of ESD. Note the peak at 5

Another important geometrical parameter is the number of the sides of individual faces on the polyhedron. If the mean number of the face is given, the mean number of the side of individual faces can be derived theoretically. According to Euler's theorem of the polyhedron, there is the following general relation

$$F-E+C=2, \tag{1}$$

where F, E and C are the numbers of faces, edges and corners of a polyhedron, respectively. An edge on any polyhedron connects always two corners. To the polyhedron of ESD there is an additional restriction that a corner is made by three edges. Consequently,

$$3C=2E \tag{2}$$

is derived. This relation together with (1) leads to

$$E=3(F-2). \tag{3}$$

Every edge is shared by two neighbouring faces, and the mean number $\bar{e}$ of the sides of a face is then

$$\bar{e}=2E/F, \tag{4}$$

and if F is 14, (3) and (4) give

$$\bar{e}=72/14=5.14.... \tag{5}$$

The result suggests the predominance of pentagon, and it is really confirmed by observation on the mathematical model as demonstrated in Fig. 5. The frequent appearance of pentagons on the polyhedra of ESD plays an important role in determining the shape of vascular trees which will be discussed in the proper place.

ESD Under Polarized Force

Three-dimensional ESD is incompatible with uneven force, and any polarization in the field of force causes ESD of lower dimensions. In this section the effect of polarized force on ESD is analyzed on a simple model.

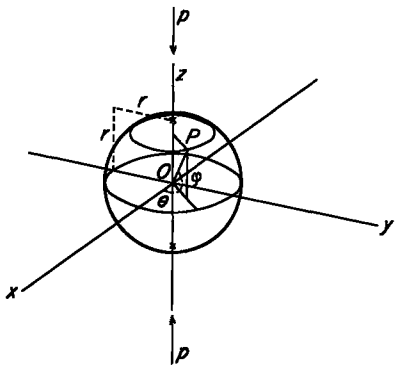

Fig. 6. Spherical cell aggregate and the orthogonal co-ordinate system O-xyz to define the position of a cell on the sphere surface. The co-ordinates of the cell can also be expressed by the following three parameters. r: radius of the sphere, θ: angle of rotation from the x-axis, ϕ: angle of inclination against the x-y plane

Suppose a spherical cell aggregate packed under uniform centripetal force and take an orthogonal co-ordinate system $O-xyz$ with O placed at the sphere center as in Fig. 6. From this state the constituent cells are allowed to proliferate uniformly under additional pressure p superimposed in the direction of the z-axis. Because the transformation of this cellular mass will be the same in every direction around the z-axis, an analysis on the $x-z$ plane alone gives sufficient information about the shape of the total structure. Let the co-ordinates of a cell on the surface of the aggregate on the $x-z$ plane be x and z after a lapse of time t. The growth of the cell heap, if the compressive effect of p is disregarded, is defined by

$$\frac{1}{x}\frac{dx}{dt}=g \tag{6}$$

and

$$\frac{1}{z}\frac{dz}{dt}=g, \tag{7}$$

where g is a parameter and may be called growth factor.

On the other hand, the cell aggregate is compressed by p. The transformation due to this extraneous force, when the cells cease to proliferate, is not associated with a change in the volume of the structure. A cylinder with circular faces of x in radius and a height of z is supposed in the cell aggregate. The condition that its volume v does not change with t is then

$$\frac{dv}{dt}=\frac{d}{dt}(\pi x^2 z)=0, \tag{8}$$

and the following relation is further derived from this.

$$\frac{1}{z}\frac{dz}{dt}=-\frac{2}{x}\frac{dx}{dt}. \tag{9}$$

With a parameter k depending upon the plasticity of the cell heap, which may be called plasticity factor, (9) is expressed as

$$\frac{1}{x}\frac{dx}{dt}=kp \tag{10}$$

and

$$\frac{1}{z}\frac{dz}{dt}=-2kp. \tag{11}$$

Because cell proliferation and compression are independent of each other, the transformation of the growing cell heap under polarized force is given by (6) +(10) and (7)+(11), so that the results are

$$\frac{dx}{dt}=(g+kp)x \tag{12}$$

and

$$\frac{dz}{dt}=(g-2kp)z. \tag{13}$$

The solution of these differential equations are

$$x=r\cos\phi\cdot\exp(g+kp)t \tag{14}$$

and

$$z=r\sin\phi\cdot\exp(g-2kp)t, \tag{15}$$

where r is the radius of the original spherical cell aggregate and ϕ is the angle of inclination of the line connecting a cell on the surface of the structure with O against the x–y plane: $r\cos\phi$ and $r\sin\phi$ give accordingly the initial conditions of differential equations.

In the case of $p>0$ or if p has compressing effect, the initial spherical structure becomes more and more flattened with the lapse of time and approaches to a disc on the x–y plane, and in the range of $g-2kp<0$ or under relatively slow cell proliferation a two-dimensional structure will be produced in a sufficiently long time. An example is demonstrated in Fig. 7. The same result is also obtained under uniform centrifugal force around the z-axis.

An entirely different structure is produced in the case of $p<0$ or if p is force drawing the cell aggregate along the z-axis. The initial spherical structure is elongated into a spindle-shaped one, and under a condition of $g+kp<0$ or relatively slow cell proliferation the final result will be a one-dimensional thread-like structure. Centrifugally acting p along the z-axis can also be replaced by uniform centripetal force toward the z-axis.

Actual histological structures may correspond to some intermediate stages from three-dimensional to lower-dimensional structures. Within them the cellular arrangement is influenced by the

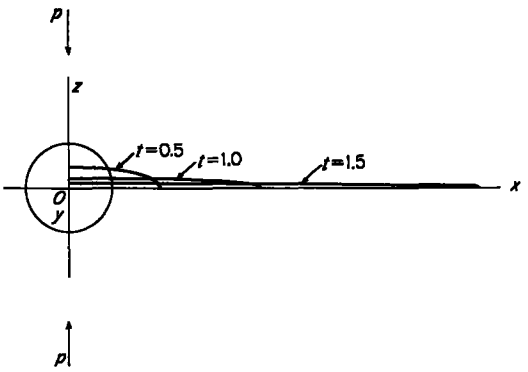

Fig. 7. Transformation of the cell aggregate of Fig. 6 growing under polarized force is calculated from (14) and (15) with $g=0.5$, $k=1$ and $p=1$

plasticity of cell bodies and the adhesiveness of cell surfaces. In a thin plate, for example, it may have an alignment of relatively tall columnar cells or may still preserve multiple layers of flattened cells. In the former case plastic resistance must be larger than the resistance to mutual dislocation of cells along their surfaces, and in the latter the relation of the two physical properties would be reversed.

The present analysis on a simple model reveals a possibility of deriving manifold aspects of supracellular structures mainly out of the conditions of the field of force. Such an approach to morphogenesis is supported by the finding of three-dimensional supracellular structures. They are completely compatible with the universal physical principle. Except for possible variations due to difference in the physical properties of cell bodies and cell surfaces it would be impossible to assume any biological activity specific and intrinsic to living cells which would determine their arrangement in the space.

It is thus concluded that there is only one structural principle underlying all the supracellular structures including pathological ones, in spite of their manifold and highly divergent appearances. The principle is ESD under a variety of the fields of extraneous mechanical force and subordinate to the second law of thermodynamics minimizing the potential energy of the system of structural units.

Supracellular Structural Principle and Its Application to an Analysis of the Vascular System

The structural principle of cell aggregates and larger supracellular units is essentially a stochastic one under some mechanical restriction. This clearly demonstrates that a completely deterministic derivation of the structures of the multicellular organism form the "code" of DNA molecules is impossible. Supracellular structures would not be perfectly identical even among the "cloned" individuals, because some freedom is always inherent to them.

If a large number of structural constituents are distributed in the space in an entirely stochastic process, they will disperse into a random distribution or into a state of complete disorder devoid of any structure. However, they will precipitate a certain structure, if the stochastic process proceeds under some mechanical restriction. The resulting structure may be quite a definite one or it may be still free in some aspects. In any case, the final structure

has to minimize the potential energy of the system in the field of force. The conclusion provides the fundamental theoretical basis for a morphological analysis of supracellular structures of multicellular organisms.

From this consideration it is further anticipated that there would be anatomical structures which are essentially dependent upon ESD but not immediately subordinate to genetic information. The problem will be most effectively examined on the vascular system.

The general design of three-dimensional supracellular structures is that the polyhedra of ESD made of parenchymal masses are separated by connective tissue septa of variable extension. Blood vessels are found in the connective tissue septa. In special cases blood space may occupy the greater part of some faces of the polyhedra of ESD as in Fig. 1d. In the majority of biological structures, however, blood vessels are predominantly localized in the region around the edges of the polyhedra. This particular tendency is most remarkable in the distribution of capillaries around relatively small structural units as in Fig. 1b, but it is still obvious in larger vascular branches. It is apparently due to the more or less plastic nature of biological structural units. When soft spheres are compressed by extraneous force and transformed into polyhedra, the spaces around the edges are not easily obliterated by compression and persist as blood vessels. If each polyhedron is replaced by a node and every two nodes corresponding to two contacting polyhedra are connected with a branch, the node-branch system makes a network, which is conjugate with one constituted by the edges of polyhedra. Consequently, it is expected that the geometry of blood vessels would reflect ESD.

A proper approach to the problem should be a statistical one in view of the nature of this particular space division. However, such a theoretical treatment would not be practicable without very complicated calculations, even if it is possible. For the purpose of easy perspective a simpler model is introduced into the following analyses. It is a trial to replace ESD with a complete space division with uniform polyhedra preserving the local topological characters of ESD that three faces unite to an edge and four edges converge to a corner. The result does not reproduce the metric properties of ESD, but it may still be regarded as a useful approximation to ESD.

Block Model

The preliminary step is to make a pile of uniform rectangular hexahedra, which are simply called blocks. The blocks are arranged in the same orientation and aligned into rows. A number of rows are then placed side by side to make a plate in such a way that any border of the blocks in a row does not join with ones of the neighbouring rows. A number of plates are further so piled one upon another that any border of the blocks in a plate does not extend into one of the two contiguous plates. The principle of the design of block pile is demonstrated in Fig. 8. It is then assumed that the line delineated by a border of blocks on the faces of their neighbours produces a new edge on the latter. As a result every block represents a polyhedron with more than

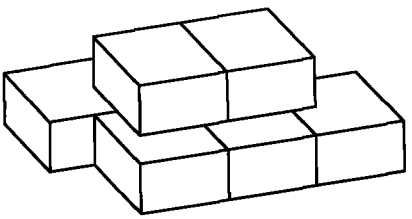

Fig. 8. A pile of blocks is presented showing the mutual relation of the borders of blocks

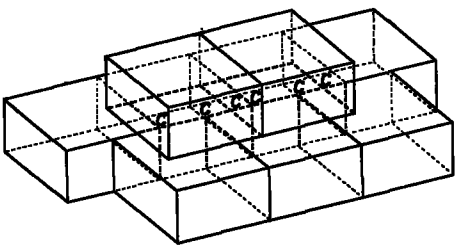

Fig. 9. Local topological conditions of ESD are reproduced by the block model. Note four edges converging to every *C*. It is also possible to notice three faces making an edge

six faces, and the heap of polyhedra defined in this way from the block pile is called "block model" in the present study. It reproduces the local topological conditions of ESD perfectly: every edge is made by three faces and every corner by four edges as demonstrated in Fig. 9.

The next step is the application of topological transformation to the block model. In this process metric geometrical properties are allowed to change freely. The faces may be changed from planes to curved surfaces. The angle made by faces at an edge and the length and shape of edges are also susceptible of change without restriction. This means that new edges delineated on the faces of blocks are protruded into the space to make "real" edges of polyhedra. We can suppose the transformation that real polyhedra, folded once in the form of the block model, are inflated and allowed to resume their original shapes. The topological properties including the number of faces on each polyhedron are kept unchanged in this process. Through this transformation the block model is changed into a pile of polyhedra which completely fill the three-dimensional space.

Another restiction is now imposed upon the shape of the block, and the ratio of its length in the direction of the row and breadth is fixed to 2:1. The height of the block may be left free. In this case two different types are possible in piling up the block plates. In one of them the plates are so placed that the rows of blocks are all parallel. In the other the directions of the rows in every two contacting plates cross perpendicular to each other. The former is called α-type and the latter β-type. They are diagrammatically presented in Fig. 10. The shapes of all the polyhedra are the same within each type, because the mutual positional relation of the blocks is the repetition of one and the same pattern.

The block model realizes a space division with uniform polyhedra, and the polyhedron is tetrakaidecahedron regardless of the difference in the type

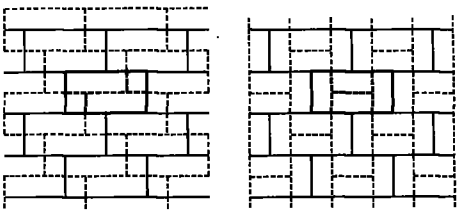

Fig. 10. Two types of block models corresponding to complete space division with uniform polyhedra are demonstrated. Solid and broken lines stand for every two different block plates laid one upon the other. Thick lines delineate a block. Four faces are noticed on a block on the plane of the figure in both types of block models. Four faces on each of the upper and lower surfaces of a block make eight faces, and on the sides of a block six faces are present. Consequently, every block has 14 faces

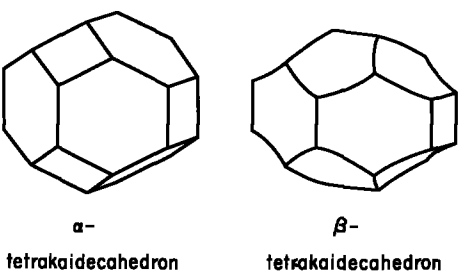

Fig. 11. Two types of tetrakaidecahedra derived from the block models of Fig. 10 are presented. Their metric properties are susceptible of change. For example, their heights may be changed freely without affecting their characteristic of ensuring complete space division. The angle made by two neighbouring hexagonal faces of a β-tetrakaidecahedron is also indefinite

of the model. It demonstrates at the same time that a complete space division with uniform polyhedra preserving the local topological characteristics of ESD is possible only with tetrakaidecahedra. The result is important in association with the observation on the polyhedra of ESD that the mean number of their faces is approximately 14. The geometrical shape of the constituent polyhedra is, however, different according to the two types of the block model. The polyhedron of the α-type block model is called α-tetrakaidecahedron and that of the β-type β-tetrakaidecahedron. In Fig. 11 examples of both polyhedra are shown for comparison.

An α-tetrakaidecahedron has 8 hexagonal, 4 parallelogrammic and 2 rectangular faces. All the faces are planes. Its typical example is Kelvin's tetrakaidecahedron, which was reported by Kelvin (W. Thomson) in 1887 in his study of space division with soap foam and has equal edges. It had been believed to be the only polyhedron which could completely fill the space preserving the local topological conditions of ESD, until Williams found in 1968 the β-tetrakaidecahedron which could also be used for the same purpose. It has 8 pentagonal, 4 hexagonal and 2 rectangular faces. Except for the last ones all the faces are curved and correspond to cylindrical surface.

As pointed out by Williams, this particular polyhedron is a better approximation to ESD than Kelvin's tetrakaidecahedron, because the former has pentagonal faces, which are completely absent on the latter. Frequent incidence of pentagonal faces is not only ascertained for example by observation on plant cells, but it is theoretically expected from (5). Apart from this reason, incorporation of faces with odd numbers of sides into the model of space division is indispensable for the analysis of vascular geometry, which is to be discussed

in the next section. Accordingly, only the model of β-tetrakaidecahedron is acceptable in the present study.

Geometrical Parameters of Arteries

Suwa et al. (1963) and Suwa and Takahashi (1971) demonstrated that blood flow Q of an arterial branch of r in radius could be expressed as a function of arterial radius in the form of

$$Q=qr^n, \tag{16}$$

in which q and n were parameters. They also found that the expected length l of an arterial branch of r in radius was given by

$$l=hr^i, \tag{17}$$

in which h and i were parameters. The exponent n in (16) corresponds to „Verzweigungsexponent" of Thoma (1901) and has a value between 2.6 and 2.7. It is influenced neither by the difference of arterial systems nor by the size of arterial branches. The values of i in (17) are about 1.2 to 1.4 in the majority of arterial systems as demonstrated in Table 1. In particular arteries, however, i deviates more or less from this range. The reason for the deviation will be discussed later, and in this connection the standard value of i may be regarded as not much different from 1.3.

With these experimental results it is possible to estimate the blood pressure drop of an arterial branch. The classical Poiseuille expression is

$$\Delta P=8\eta Ql/\pi r^4, \tag{18}$$

where ΔP is the blood pressure difference between both ends of an arterial branch of l in length and r in radius, through which steady laminar flow Q of blood with a viscosity coefficient η is maintained. The expression is transformed with (16) and (17) into

$$\Delta P=(8\eta/\pi)qhr^{n+i-4}. \tag{19}$$

Expression (19) indicates the importance of combined effects of n and i on blood circulation. In the following part of this section attempts are made to derive the values of the two parameters from the geometry of ESD, partly with the aid of space division with uniform β-tetrakaidecahedra.

From a purely geometrical viewpoint blood vessels should develop in the space along the edges of ESD, and the division of vascular trees at a corner should be trichotomy, because four edges converge to a corner. In reality, however, dichotomy is clearly predominant in every vascular system from its large branches to capillaries. Consequently, there must be some mechanism which would exclude vascular branches on one-fourth of the edges of ESD, and it is realized by introduction of a rheological factor into the geometry of ESD.

Table 1. Experimental values of i

Artery or organ	Estimated i	Confidence interval of i at 95% level
Mesenteric artery	1.33	1.29–1.37
Femoral artery	1.17	1.13–1.21
Cerebral cortex	1.35	1.32–1.38
Coronary artery	1.20	1.15–1.25
Pulmonary artery	1.29	1.24–1.35
Renal artery	1.03	1.00–1.07
Cerebral basal ganglia	1.79	1.71–1.87

The values of i are calculated as the regression coefficient of orthogonal mean square regression of log r and log l.

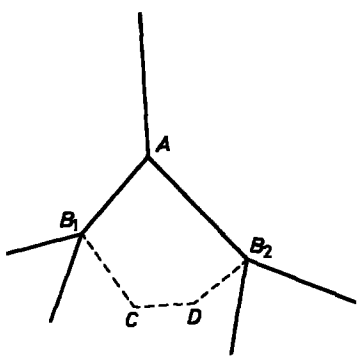

Fig. 12. Dichotomic vascular tree on edges of ESD. Deflected broken line shows a possible route on edges of ESD available for blood stream, if the blood pressure levels at B_1 and B_2 are different

A vascular branch is now supposed to be on an edge of ESD as in Fig. 12. It divides at a corner A into two sub-branches situated on two diverging edges and reaching the next corners B_1 and B_2. The sub-branches AB_1 and AB_2 divide again at B_1 and B_2 each into two smaller sub-branches. The dichotomic design of the vascular tree leaves free a connection between B_1 and B_2 via edges of ESD. If blood pressure drops along the sub-branches AB_1 and AB_2 are different, blood pressure levels at B_1 and B_2 are also different, and a new channel for blood stream will be opened along the edges connecting B_1 and B_2. Trichotomy will thus develop at these two corners. In order to sustain dichotomy blood pressure drops of the two sub-branches must be equal, even if they are of different sizes. Mathematical expression for this condition is derived from (19) as

$$n+i-4=0. \tag{20}$$

Another condition is still necessary to make possible dichotomic design of blood vessels on the edges of ESD. It is the presence of faces with odd numbers of sides, the effect of which is visualized in Fig. 13. Blood is let flow into the routes along the sides of a polygon from one of its corners. In a polygon with an odd number of sides blood pressure levels at both ends of

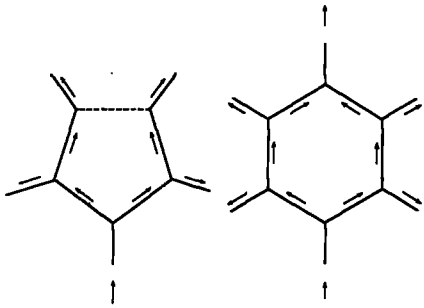

Fig. 13. The routes of blood stream along the sides of a pentagon is contrasted to those of a hexagon. The directions of blood stream are indicated by arrows. Blood pressure drops along individual sides are assumed to be equal. Broken line shows the edge on which blood stream does not develop

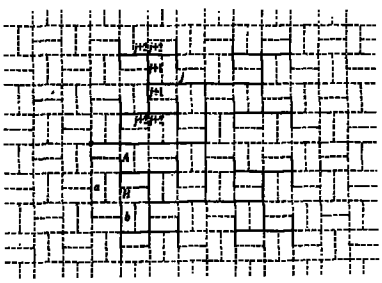

Fig. 14. A dichotomic vascular tree is designed on edges of a plate of the β-type block model. Broken lines show the edges potentially available for the design and solid lines used ones. Each terminal of the branching system corresponds to a block. For example, two terminals *A* and *B* are respectively coupled with two blocks *a* and *b* delineated with thick broken lines. The step of ramification is expressed with *j*. An identical design is possible on every block plate, so that the result is the arrangement of dichotomic vascular trees with their terminals uniformly distributed in the three-dimensional space

the side opposite to the corner of blood inflow are equal. A blood stream cannot develop along this side and the route is excluded from the circulation. In contrast, such an effect is not brought about by a polygon with an even number of sides. Predominant dichotomy in the vascular system can thus be intepreted in association with the frequent incidence of pentagonal faces in ESD.

Expression (20) has two variables n and i, so that another equation is necessary to determine their values. This is given by the model of space division with uniform β-tetrakaidecahedra, which is expected approximately to substitute for ESD. An attempt is now made to design a progressively dichotomic system simulating the vascular tree on some edges of this model, under the condition of ensuring one-to-one correspondence of the terminal branches to constituent polyhedra. The condition is required to reproduce uniform distribution of the vascular terminals in the space. The analysis is preferably made directly on the β-type block model for easy perspective, because all the edges used for the branching system change their length uniformly in topological transformation from the block model to the pile of β-tetrakaidecahedra. The only possible design of the ramification is demonstrated in Fig. 14.

The most noteworthy characteristic of this dichotomic system is that the length of the branch is reduced to a half at every second division. The relation is expressed by

$$l_j = 2l_{j+2}, \tag{21}$$

the subscripts denoting the steps of ramification. The expression is transformed with (17) into

$$r_j^i = 2r_{j+2}^i. \tag{22}$$

On the other hand

$$r_j^n = 2r_{j+1}^n = 4r_{j+2}^n \tag{23}$$

is derived from (16), because a branch divides into two equal sub-branches on this model. From the comparision of (22) and (23)

$$2i = n \tag{24}$$

is obtained. This relation gives in combination with (20)

$$n = 8/3 = 2.66 \ldots \tag{25}$$

and

$$i = 4/3 = 1.33 \ldots \tag{26}$$

The agreement of the results with those of observation may be regarded satisfactory.

The present theoretical treatments, however, depend partly on a model of space division which can only approximately substitute for ESD, but not directly on ESD itself. In this respect they should be further improved by exploration of mathematical analysis based on some statistical theory. At present, however, such an approach seems to be very difficult, if it is not utterly impossible.

This section will be concluded with brief comments on the deviations of i in some arteries. In this connection the renal artery and the arteries of the cerebral basal ganglia are taken into consideration. The renal artery has a value of i significantly lower than that of standard arteries. The deviation would most reasonably be attributed to the particular growth pattern of the kidney. In Fig. 15 the kidney from a normal adult is contrasted to a fetal kidney. It is clearly demonstrated that postnatal growth of this organ is accompanied by remarkable volume increase of renal tubules, which widely exceeds the enlargement of glomeruli. This inevitably causes an accentuated elongation of terminal renal arterioles and contributes to lowering i.

A deviation of i in the opposite direction is found in arteries of cerebral basal ganglia. An extremely high value of i is most probably due to remarkable postnatal development of cerebral cortex in contrast to the growth of basal ganglia. This will lead to excessive elongation of proximal arterial branches.

It is very likely that in early stages of blood vessel development in fetal life n and i are completely subordinate to the geometrical restriction of ESD and their values are common to

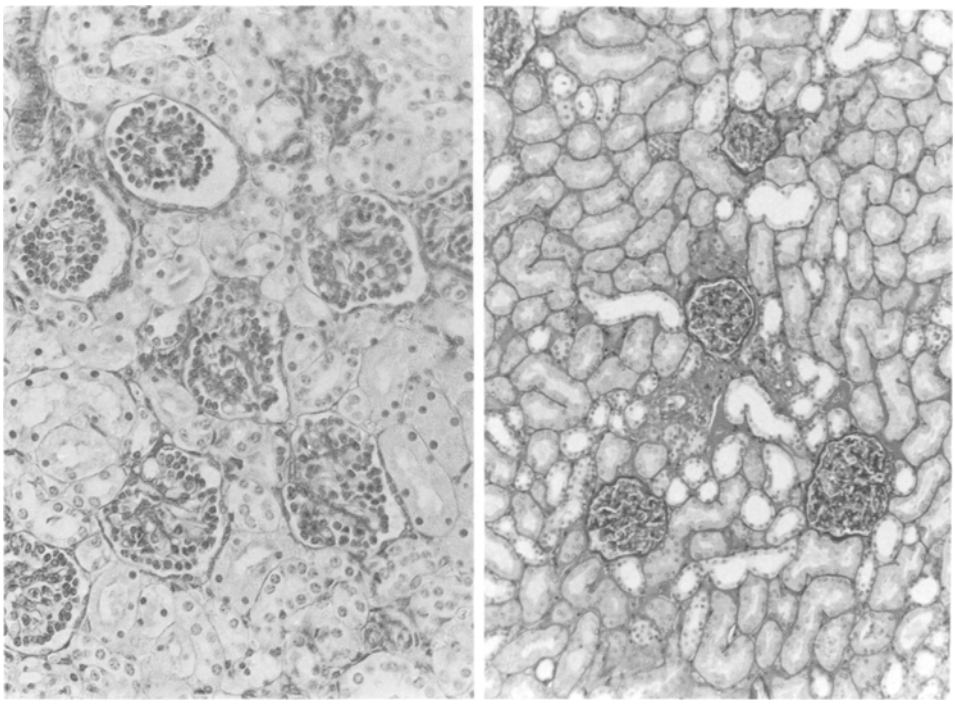

Fig. 15. Normal fetal *(left)* and adult *(right)* kidneys are demonstrated for comparison. Note remarkable increase in the volume of renal tubules in the adult kidney. Fetal kidney is presented under a higher magnification

all the organs. The adaptation of arteries to specific growth pattern of organs is achieved only by changing i, while n is not influenced.

Comments

The supracellular structures of a multicellular organism are produced essentially by a stochastic process under incomplete mechanical restriction. The constituent units are merely piled in an arrangement required from the second law of thermodynamics to minimize the potential energy of the system, just as inorganic materials are packed under extraneous force. This leads to a particular space division or to ESD, which is the only principle of all the supracellular structures including pathological ones, in spite of their extremely variable appearances.

Even living cells and larger structural units are not capable of definitely prescribing the position of their neighbours in the space. In this respect the structural principle of the multicellular organisms is fundamentally different from that of crystals, in which the positions of constituent atoms in the space is definitely determined by interatomic force. There is practically no freedom in the structural design, and extraneous force does not exert any essential effect on crystalline structure.

It is consequently impossible to attribute the development of supracellular

biological structures entirely to the template function of DNA molecules. This concept of molecular biology is only compatible with deterministic thinking and cannot be immediately extended and applied to morphogenesis beyond the cell level. Genetic information may direct cell proliferation and differentiation and participate in the formation of a field of mechanical force. After the situation is established, however, biological structures are no longer brought to existence through a deterministic mechanism. This mechanism must be replaced by stochastic processes under incomplete restrictions.

It is anticipated from this consideration that there are some structural parameters depending upon ESD but not directly upon genetic determination. Geometrical parameters n and i of blood vessels are derived from this viewpoint in good agreement with the experimental results. It may also be predicted that the two parameters will prove to have values common to all animal species.

The present study is an attempt to provide a theoretical basis for the morphological analysis of supracellular structures. It may contribute to establishing a method with which the manifold appearances of biological structures can be derived from a common physical principle applicable to organisms as well as to inorganic materials.

References

Bernal JD (1959) A geometrical approach to the structure of liquids. Nature 183:141–147

Bernal JD (1964) The structure of liquids. The Bakerian Lecture, 1962. Proc R Soc Lond A 280:299–322

Bernal JD, Mason J (1960) Co-ordination of randomly packed spheres. Nature 188:910–911

Dodd JD (1944) Three-dimensional cell shape in the carpel vesicles of *Citrus grandis*. Am J Bot 31:120–127

Finney JL (1970) Random packings and the structure of simple liquids. I. The geometry of random close packing. Proc R Soc Lond A 319:479–493

Gotoh K and Finney JL (1974) Statistical geometrical approach to random packing density of equal spheres. Nature 252:202–205

Lewis FT (1923) The typical shape of polyhedral cells in vegetable parenchyma and the restoration of that shape following cell division. Proc Am Acad Arts Sci 58:537–552

Marvin JW (1939) The shape of compressed lead shot and its relation to cell shape. Am J Bot 26:487–504

Matzke EB (1939) Volume-shape relationships in lead shot and their bearing on cell shapes. Am J Bot 26:288–295

Matzke EB (1946) The three-dimensional shape of bubbles in foam – an analysis of the role of surface forces in three-dimensional cell shape determination. Am J Bot 33:58–80

Suwa N, Niwa T, Fukasawa H, Sasaki Y (1963) Estimation of intravascular blood pressure gradient by mathematical analysis of arterial cast. Tohoku J Exp Med 79:168–198

Suwa N, Takahashi T (1971) Morphological and morphometrical analysis of circulation in hypertension and ischemic kidney. Urban & Schwarzenberg, München-Berlin-Wien

Thoma R (1901) Über den Verzweigungsmodus der Arterien. Arch Entwicklungsmechanik 12:352–414

Thomson W (1887) On the division of space with minimum partitional area. London, Edinburgh, Dublin Phil Mag J Sci 24:503–514

Williams RE (1968) Space-filling polyhedron: its relation to aggregates of soap bubbles, plant cells and metal crystallites. Science 161:276–277

Accepted August 28, 1980